AD-A062 293 NATIONAL BUREAU OF STANDARDS WASHINGTON DC SURFACE S--ETC F/G 7/4
CATALYTIC DECOMPOSITION OF FORMALDEHYDE ON SINGLE RHODIUM ATOMS--ETC(U)
NOV 78 J T YATES, S D WORLEY, T M DUNCAN N00014-78-F-0008

UNCLASSIFIED TR-9 NL

| OF |
ADA
062293

END
DATE
FILMED
3 -79
DDC

OFFICE OF NAVAL RESEARCH
Contract N00014-78-F-0008

Technical Report

Catalytic Decomposition of Formaldehyde on Single Rhodium Atoms

by

J. T. Yates, Jr.*, S. D. Worley†, T. M. Duncan, and R. W. Vaughan

Department of Chemistry and Chemical Engineering
California Institute of Technology
Pasadena, California 91125

November 1, 1978

To be published in the Journal of Chemical Physics

* Sherman Fairchild Distinguished Scholar, on leave from the National Bureau of Standards, Washington, DC 20234.

† Visiting Guest Worker. Permanent address: Department of Chemistry, Auburn University, Auburn, Alabama 36830

UNCLASSIFIED

SECURITY CLASSIFICATION OF THIS PAGE (When Data Entered)

REPORT DOCUMENTATION PAGE

READ INSTRUCTIONS BEFORE COMPLETING FORM

1. REPORT NUMBER (14) TR-
Technical Report No. 9

2. GOVT ACCESSION NO.

3. RECIPIENT'S CATALOG NUMBER

4. TITLE (and Subtitle) (6)
Catalytic Decomposition of Formaldehyde on Single Rhodium Atoms ,

5. TYPE OF REPORT & PERIOD COVERED (9)
Interim technical rept.

6. PERFORMING ORG. REPORT NUMBER

7. AUTHOR(s) (10)
J. T. Yates, Jr., S. D. Worley, T. M. Duncan and R. W. Vaughn

8. CONTRACT OR GRANT NUMBER(s) (15)
N00014-78-F-0008

9. PERFORMING ORGANIZATION NAME AND ADDRESS
Surface Science Division
National Bureau of Standards
Washington, DC 20234

10. PROGRAM ELEMENT, PROJECT, TASK AREA & WORK UNIT NUMBERS

11. CONTROLLING OFFICE NAME AND ADDRESS (11)
Office of Naval Research
Physical Program Office
Arlington, VA 22217

12. REPORT DATE
1 Nov 78

13. NUMBER OF PAGES

14. MONITORING AGENCY NAME & ADDRESS (if different from Controlling Office) (12) 26p.

15. SECURITY CLASS. (of this report)
Unclassified

15a. DECLASSIFICATION/DOWNGRADING SCHEDULE

16. DISTRIBUTION STATEMENT (of this Report)

Approved for Public Release; Distribution Unlimited.

17. DISTRIBUTION STATEMENT (of the abstract entered in Block 20, if different from Report)

18. SUPPLEMENTARY NOTES

Preprint; to be published in the Journal of Chemical Physics.

19. KEY WORDS (Continue on reverse side if necessary and identify by block number)

Adsorbate structure; carbonyl hydride species; carbon monoxide; formaldehyde; formyl; rhodium.

20. ABSTRACT (Continue on reverse side if necessary and identify by block number)

The interaction of H_2CO with alumina-supported Rh has been studied by transmission infrared spectroscopy. It has been shown that isolated Rh atoms catalyze the decomposition of H_2CO to produce carbonyl hydride species $H_x Rh(CO)_2$ (x = 1,2). Species of the type Rh(HCO) and Rh(HCOH) are not observed to form in detectable amounts. Hydride bonding to rhodium carbonyl species is associated with electron donation to Rh causing a decrease in ν_{CO} due to → next page

(Continued on reverse side)

ν_{CO} sub CO

DD FORM 1 JAN 73 1473 EDITION OF 1 NOV 65 IS OBSOLETE
S/N 0102-014-6601

UNCLASSIFIED

SECURITY CLASSIFICATION OF THIS PAGE (When Data Entered)

78 12 11 060

410 655

2 pi*

electron donation into $2\pi^*$-CO orbitals. Hydride displacement by CO may occur on exposure to CO(g). The conversion of the species $H\text{-}Rh(CO)_2^-$ to $H\text{-}Rh(CO)$ has been followed spectroscopically during desorption.

Catalytic Decomposition of Formaldehyde on Single Rhodium Atoms

by

J. T. Yates, Jr.*, S. D. Worley**, T. M. Duncan, and R. W. Vaughan

Division of Chemistry and Chemical Engineering
California Institute of Technology
Pasadena, California 91125

* Sherman Fairchild Distinguished Scholar, on leave from NBS, Washington, D.C. 20234. To whom all correspondence should be addressed.

** Visting guest-worker. Permanent address: Department of Chemistry, Auburn University, Auburn, Alabama 36830.

Abstract

The interaction of H_2CO with alumina-supported Rh has been studied by transmission infrared spectroscopy. It has been shown that isolated Rh atoms catalyze the decomposition of H_2CO to produce carbonyl hydride species H_xRh-CO (x = 1,2). Species of the type Rh(HCO) and Rh(HCOH) are not observed to form in detectable amounts. Hydride bonding to rhodium carbonyl species is associated with electron donation to Rh causing a decrease in $\tilde{\nu}_{CO}$ due to electron donation into $2\pi^*$-CO orbitals. Hydride displacement by CO may occur on exposure to CO(g). The conversion of the species H-Rh$(CO)_2$ to H-Rh(CO) has been followed spectroscopically during desorption.

I. Introduction

In a previous paper[1] we have used infrared spectroscopy to characterize the chemisorption of CO on highly dispersed Rh atoms supported on high-area Al_2O_3. This work forms a foundation for the present study of formaldehyde chemisorption on similar Rh surfaces.

Rh is a very active catalyst for the production of CH_4 from H_2 + CO, the catalytic methanation reaction[2-4]. It has been postulated[2] that intermediates such as HCO(ads) or HCOH(ads) may be involved in catalytic methanation. Therefore, in this work a spectroscopic search for these species was undertaken using H_2CO as the adsorbate. In related work on single crystals of W and Ru, it has been observed that small quantities of CH_4 are produced by thermal desorption following adsorption of H_2CO[5-10]. Both W and Ru are active catalysts for the methanation reaction[11,2], and the observation of CH_4 production from H_2CO has given support to the hypothesis that intermediates derived from H_2CO may also be present in the reaction of H_2 + CO to yield CH_4.

The chemisorption of H_2CO by metals has been previously studied[5-14], but no definitive vibrational spectroscopic work has been reported for surface species derived from this molecule.

II. Experimental

The experimental apparatus and the infrared spectrometer have been described previously[1]. Highly dispersed Rh supported on Al_2O_3 was prepared as described earlier[1,4] by reduction of highly dispersed $RhCl_3$ on Al_2O_3 using H_2 at 150° C. $H_2CO(g)$ was prepared[5] by heating paraformaldehyde in a glass generator at 80° C, passing the gas through a glass trap at 195 K, and directly admitting the $H_2CO(g)$ to the stainless steel manifold. At H_2CO pressures as high as 5 torr, little

difficulty was encountered with polymerization loss at the vacuum system walls as judged by the constancy (~2%) of $H_2CO(g)$ pressure in the isolated manifold for times of the order of minutes. This method of producing $H_2CO(g)$ from paraformaldehyde has been checked mass-spectrometrically and was found to produce pure H_2CO[5]. $D_2CO(g)$ was prepared as above from completely deuterated paraformaldehyde obtained from Merck Isotopes.

III. Experimental Results

A. H_2CO Adsorption of Rh

Figure 1A shows the spectral developments which occur as successive quantities of H_2CO are adsorbed on Rh. It may be seen that at lowest H_2CO exposures a band near 1860 cm^{-1} and a band near 2038 cm^{-1} develop. As the H_2CO exposure is increased, there is an indication of three overlapping features at 2026 cm^{-1}, 2048 cm^{-1}, and 2066 cm^{-1}, as well as a small sharp band near 2100 cm^{-1}. This spectrum is distinctly different from the spectrum of ^{12}CO on Rh (see reference 1, Figure 3), where a strong doublet feature at 2101 cm^{-1} and 2031 cm^{-1} is dominant at comparable levels of CO exposure.

It was important to determine whether Rh was acting as a catalyst for decomposition of $H_2CO(g)$ into $H_2(g)$ and $CO(g)$. If this were true, then the spectra of Figure 1A could be attributed to competition between $H_2(g)$ and $CO(g)$ for adsorption sites, and the absence of the doublet feature obtained with pure CO could be attributed to this competition. Therefore, the experiment shown in Figure 1A was repeated on a freshly prepared Rh surface using an equimolar H_2+CO mixture instead of $H_2CO(g)$ as the adsorbate. The results are shown in Figure 1B where the dosage of the H_2 + CO mixture has been made equivalent to the $H_2CO(g)$ dosage used in Figure 1A for each spectrum, a through e. Spectral developments using the H_2 + CO mixture are very similar to those observed for pure CO

adsorption. The major differences observed in comparison of the spectra in Figures 1A and 1B indicate that $H_2CO(g)$ does not behave in a fashion resembling $H_2(g) + CO(g)$ during chemisorption on Rh.

Since the doublet feature characteristic of pure CO adsorption on Rh was strongly retarded in its development with H_2CO as the adsorbing species, we attempted to see whether the doublet would develop by adsorbing CO following high exposures of H_2CO on Rh. This procedure caused the development of new spectral features as shown in Figure 2. Extensive development of the doublet occurs as well as some growth of features at ~2060 cm^{-1} and 1880 cm^{-1}.

B. D_2CO Adsorption on Rh

In order to determine whether hydrogen motions exist in any of the vibrational features observed as a result of H_2CO adsorption, the adsorption of D_2CO was undertaken. These results are given in Figure 3 where the D_2CO dosages are equivalent to those used for H_2CO in Figure 1A. There is no difference in the D_2CO and the H_2CO-derived spectra. The agreement between the frequencies for H_2CO-and D_2CO-derived species proves that the adsorbed species observed here do not involve hydrogen bonded to either C or O.

C. Desorption from Rh Exposed to D_2CO

Previous studies have shown that thermal desorption from pure CO layers on Rh is entirely reversible at $T \leq 336$ K[(1)]. A similar study was performed on a Rh surface which had been exposed to D_2CO. The results shown in Figure 4 are strikingly different from the pure CO results since an interconversion between different adsorbed species is indicated by the significant increase in absorbance near 2048 cm^{-1} as the doublet features at ~2090 cm^{-1} and ~2018 cm^{-1} disappear during desorption. In the lower portion of Figure 4,

difference spectra are presented which clearly show this interconversion effect.

D. Search for Other H_2CO-derived Chemisorbed Species on Rh

A comparison of the adsorption of H_2CO on Rh/Al_2O_3 and on Al_2O_3 was made in the 4000 cm^{-1} to 1000 cm^{-1} region. A number of new spectral features were detected upon exposure to H_2CO but in each case the new feature was associated with H_2CO adsorption on Al_2O_3 except for those features shown in Figure 1A.

E. Evidence for H_2 Evolution during H_2CO Chemisorption on Rh

During the H_2CO exposures which produced the spectra a - e in Figure 1A, it was noted that the pressure within the adsorption cell and the manifold did not decrease below ~20-30% of its initial value. Similar dosages of CO would have been accompanied by a pressure drop to ~5% of the initial pressure. We suspect that this behavior is due to $H_2(g)$ evolution as H_2CO is decomposed on Rh.

F. Search for Rh-H Absorption Bands Following H_2 Adsorption

Infrared spectra were measured in the 4000 cm^{-1} to 1000 cm^{-1} region with both ~50 torr and ~500 torr of H_2 above the Rh surface at 295 K. No spectral bands due to H_2 chemisorption were detected. The accuracy of these measurements is such that an absorbance change of <0.02 could have been detected easily.

IV. Discussion

A. Assignment of IR Spectral Features - Interaction of H_2CO with Rh

By virtue of the observation of several spectral features in the CO stretching region (and the lack of CH and OH bands) a tentative assignment of H_2CO-derived adsorbed species and their vibrational frequencies may be made (Table I).

We suggest that the following surface processes occur when H_2CO adsorbs on various Rh sites which are present together on the supported catalyst[1].

Isolated Rh Atom Sites

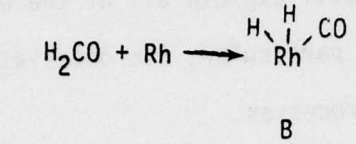

$$H_2CO + Rh \longrightarrow \underset{\text{B}}{H(H)Rh(CO)} \qquad (1)$$

Rh_x Sites

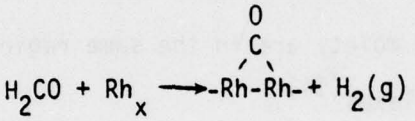

$$H_2CO + Rh_x \longrightarrow \underset{\text{III}}{-Rh(CO)-Rh-} + H_2(g) \qquad (2)$$

and

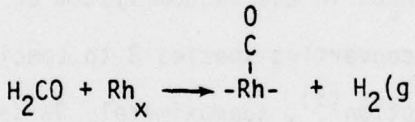

$$H_2CO + Rh_x \longrightarrow \underset{\text{II}}{-Rh(CO)-} + H_2(g) \qquad (3)$$

When additional CO is adsorbed on the Rh surface following H_2CO adsorption, the following hydrogen-displacement process takes place:

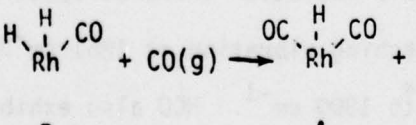

$$\underset{\text{B}}{H(H)Rh(CO)} + CO(g) \longrightarrow \underset{\text{A}}{OC(H)Rh(CO)} + \tfrac{1}{2} H_2(g) \qquad (4)$$

Finally, when thermal desorption occurs, the first step is:

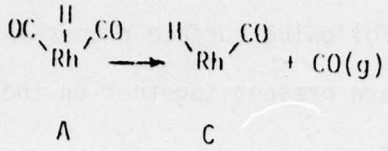

(5)

A C

This scheme of reactions will explain all of the effects observed in our experiments reported above. In particular, the observations tabulated in Table II are consistent with the above processes.

Several transition metal complexes of Rh containing the hydride and CO functional groups simultaneously, as well as other ligands, have been prepared. Thus, our proposed intermediate species A, B, and C would seem to be reasonable from a bonding point of view. It is notable that the stretching frequencies for the CO ligands and the Rh-H moiety are in the same region (ca. 2000 cm^{-1}) for these transition metal complexes[14].

It is likely that the small doublet -CO feature at 2096 cm^{-1} and 2026 cm^{-1} which was seen following exposure to $H_2CO(g)$ at ~5 torr is due to traces of CO impurity produced from the H_2CO in the vacuum system or on the Rh catalyst. This CO adsorbs via process (4) converting species B to species A. Based on control studies of CO adsorption[1], approximately 3% decomposition of H_2CO at ~5 torr would yield the doublet feature of comparable intensity to that measured in Figure 1A, spectrum e.

B. Absence of Detectable Surface Coverages of HCO(ads) or HCOH(ads)

The infrared spectra of $\dot{H}CO$ and $\dot{D}CO$ (the formyl radical) have been studied by others using matrix-isolation infrared spectroscopy[15]. For $\dot{H}CO$, a very intense CO stretching vibration at 1861 cm^{-1} was observed, whereas $\dot{D}CO$ gave a feature shifted to 1800 cm^{-1}. $\dot{H}CO$ also exhibited an abnormally low C-H stretching vibration at 2488 cm^{-1} [15].

We can eliminate HCO(ads) and HCOH(ads) as being present on Rh at 295 K in concentrations measurable by infrared spectroscopy on the following basis:

1. Evidence against HCO(ads) on Rh.

   i. No new spectral features near or below 1861 cm^{-1} were observed in comparing H_2CO with CO adsorption on Rh.

   ii. No shift in any C-O stretching vibration due to deuterium labeling of formaldehyde was observed.

2. Evidence against HCOH(ads) on Rh.

   i. No new C-H or O-H stretching vibrations were observed following H_2CO adsorption on Rh.

   ii. No shift in any C-O stretching vibration due to deuterium labeling of formaldehyde was observed.

C. Vibration of the H-Rh-CO Species - Evidence for Rhodium Carbonyl Hydride Species Derived from H_2CO

Two factors must be considered in discussing the variation of $\tilde{\nu}$-CO following the introduction of hydrogen ligands to Rh. The first of these is the mechanical effect on $\tilde{\nu}$-CO caused by bonding of hydrogen to Rh. Effects of this kind have been considered formally by Adel[16]. For the linear oscillator,

$$\underset{m_1}{Rh} \overset{k_{12}}{\text{—}} \underset{m_2}{C} \overset{k_{23}}{\text{—}} \underset{m_3}{O},$$

the addition of a hydrogen atom to m_1 may be considered to cause a change of $\Delta m_1 = 1$ amu at m_1. For the two stretching frequencies ω_{23} and ω_{12}, the fractional shifts in frequency are given by:

$$\frac{d\omega_{23}}{\omega_{23}} = \frac{\left[\frac{-k_{12}\,k_{23}}{\mu_{23}}\left(\frac{dm_1}{m_1^2}\right) - \left|(2\pi\omega_{23})^2 + (2\pi\omega_3)^2\right| \left|-k_{12}\left(\frac{dm_1}{m_1^2}\right)\right|\right]}{2(2\pi\omega_{23})^2\left[(2\pi\omega_{23})^2 - (2\pi\omega_{12})^2\right]} \qquad (6)$$

and,

$$\frac{d\omega_{12}}{\omega_{12}} = \frac{\left[\frac{-k_{12}\,k_{23}}{\mu_{23}}\left(\frac{dm_1}{m_1^2}\right) - \left|(2\pi\omega_{12})^2 + (2\pi\omega_3)^2\right| \left|-k_{12}\left(\frac{dm_1}{m_1^2}\right)\right|\right]}{2(2\pi\omega_{12})^2\left[(2\pi\omega_{12})^2 - (2\pi\omega_{23})^2\right]} \qquad (7)$$

where k_{ij} = force constant for bond stretching (dynes cm^{-1}).

ω_{12} = "metal-carbon" stretching frequency (sec^{-1}).

ω_{23} = "carbon-oxygen" stretching frequency (sec^{-1}).

ω_3 = "bending" frequency (sec^{-1}).

$$\mu_{ij} = \frac{m_i\, m_j}{m_i + m_j}$$

We assume typical values of $\omega_{12}, \omega_{23}, \omega_3$, and k_{ij} as found for metal carbonyls[17]. For $\tilde{\nu}_{23} \simeq 2000\ cm^{-1}$, $\omega_{23} \simeq 6 \times 10^{13}\ sec^{-1}$; for $\tilde{\nu}_{12} \simeq \tilde{\nu}_3 \simeq 400\ cm^{-1}$, $\omega_{12} \simeq \omega_3 \simeq 1.2 \times 10^{13} sec^{-1}$. Also, $k_{23} \simeq 17 \times 10^5$ dynes cm^{-1}, and $k_{12} \simeq 3 \times 10^5$ dynes cm^{-1}.

For Δm_1 = 1 amu, equations (6) and (7) yield $\frac{d\omega_{23}}{\omega_{23}} = -6 \times 10^{-6}$ and $\frac{d\omega_{12}}{\omega_{12}} = +8 \times 10^{-4}$. Thus, for the addition of a single H to Rh, $d\tilde{\nu}_{23} \simeq -.012\ cm^{-1}$ and $d\tilde{\nu}_{12} \simeq 0.32\ cm^{-1}$. The mechanical effect of hydrogen substitution on $\tilde{\nu}_{CO}$ is therefore entirely negligible and would not be observable. Also, a deuterium isotope effect would not be seen.

The second factor concerning hydrogen addition to Rh and the resultant changes in $\tilde{\nu}_{CO}$ is the electronic influence of H ligand(s) on Rh and hence on the CO ligand. It is generally accepted that hydrogen bound to the metal atom of a carbonyl will be electron donating[18,19]. This will reduce carbonyl

stretching parameters. Thus, σ-donation of electrons from H to Rh would be expected to increase π-donation from the metal into the antibonding $2\pi^*$-CO orbitals leading to a decrease in k_{23} and in $\tilde{\nu}_{CO}$. Such effects might be expected to yield ~10 cm^{-1} downward shifts in $\tilde{\nu}_{CO}$ based on comparison of metal carbonyls containing ligands of varying electron donating ability[20]. In each case in Table I where a Rh-carbonyl-hydride species is compared with its non-hydride counterpart, it is seen that $\tilde{\nu}_{CO}$ decreases by 5-10 cm^{-1} for each hydrogen ligand added. These significantly lower $\tilde{\nu}_{CO}$ values measured for H_2CO-derived species on Rh compared to CO-derived species on Rh leave little doubt that H_2CO adsorption on Rh yields carbonyl hydride species A, B, and C. There are many examples of analogous metal carbonyl hydride molecules of known structure[21].

D. Thermodynamic Estimate of the Energetics of the Reaction of H_2CO with a Rh Atom

An estimate of the Rh-CO and the Rh-H bond strength can be made using desorption activation energies, E_d, from Rh single crystal surfaces. For $H_2(g)$ desorption from Rh(111), $E_d^{H_2} \simeq \Delta H \simeq 19$ kcal $mole^{-1}$[22]. For CO desorption from Rh(111), $E_d^{CO} \simeq \Delta H \simeq 35$ kcal $mole^{-1}$[23]. On this basis, the bond strengths are estimated to be $E_{Rh-H} = 61.6$ kcal $mole^{-1}$ and $E_{Rh-CO} = 35$ kcal $mole^{-1}$. Therefore, for the reaction:

$$Rh + H_2CO(g) \longrightarrow \underset{B}{H_{\diagdown}\overset{H}{|}{}_{\diagup}Rh^{\diagup}CO} \qquad (8)$$

$$\Delta H_{(8)} \simeq -2E_{Rh-H} - E_{Rh-CO} + D^0_{H_2} - \Delta H^f_{H_2CO(g)} = -26.3 \text{ kcal mole}^{-1}.$$

For the reaction:

$$2Rh + H_2CO(g) \longrightarrow \underset{\displaystyle H}{\overset{\displaystyle |}{Rh}} + \underset{\displaystyle C}{H\!-\!Rh\!-\!CO} \qquad (9)$$

$$\Delta H_{(9)} \simeq -26.3 \text{ kcal mole}^{-1}.$$

For the ligand exchange process:

$$CO(g) + \underset{\displaystyle B}{H\!-\!\overset{\displaystyle H}{\overset{\displaystyle |}{Rh}}\!-\!CO} \longrightarrow \underset{\displaystyle A}{OC\!-\!\overset{\displaystyle H}{\overset{\displaystyle |}{Rh}}\!-\!CO} + \tfrac{1}{2} H_2(g) \qquad (10)$$

$$\Delta H_{(10)} \simeq E_{Rh-H} - E_{Rh-CO} - \tfrac{1}{2} D^0_{H_2} = -25.5 \text{ kcal mole}^{-1}.$$

Thus, all of the spontaneous processes observed in this work are expected to be exothermic and probably irreversible at 295 K and at the pressures employed here.

These thermodynamic estimates are inexact for two reasons:

(1) an isolated Rh atom will differ in its energetics from a Rh atom in a single crystal;

(2) additivity of bond energies is an inexact approximation.

However, for the higher values of E_{Rh-H} and E_{Rh-CO} expected for an isolated Rh atom compared to a Rh atom in a crystal, the exothermicity of processes 8. 9, and possibly 10 will increase.

V. Summary

The following features of H_2CO dissociative chemisorption on isolated Rh atoms have been found:

1. H_2CO chemisorbs dissociatively on isolated Rh atoms to produce carbonyl-hydride species containing a single CO ligand and one or two H ligands.
2. HCOH(ads) and HCO(ads) species are not observed to form from H_2CO on Rh at 295 K.
3. Hydride bonding to Rh-carbonyl species is associated with electron donation to the Rh causing a decrease in $\tilde{\nu}_{CO}$ in accordance with expectations for electron donation into $2\pi^*$-CO orbitals.
4. Hydride displacement by CO ligands may occur on Rh-carbonyl-hydride species by exposure to CO(g) at 295 K.
5. Thermal desorption from $OC\diagdown\overset{H}{\underset{|}{Rh}}\diagup CO$ involves loss of CO to yield $H\diagdown Rh\diagup CO$.
6. H_2CO interaction with supported Rh atoms involves specific bond-breaking and new bond formation which cannot be achieved by coadsorption of equimolar mixtures of H_2 and CO.

VI. Acknowledgment

The authors gratefully acknowledge support from ONR under contract N00014-77-F-0008 and N00014-75-C-0960. We thank Professor George R. Rossman for his kindness in allowing us to use his infrared spectrometer.

References

1. J. T. Yates, Jr., T. M. Duncan, S. D. Worley, and R. W. Vaughan, submitted, J. Chem. Phys.
2. G. A. Mills and F. W. Steffgan, Catalysis Rev. - Scientific Engineering 8, 159 (1973).
3. B. Sexton and G. A. Somorjai, J. Catalysis 44, 439 (1976).
4. A. C. Yang and C. W. Garland, J. Phys. Chem. 61, 1504 (1957).
5. J. T. Yates, Jr., T. E. Madey, and M. J. Dresser, J. Catalysis 30, 260 (1973).
6. J. T. Yates, Jr., N. E. Erickson, S. D. Worley, and T. E. Madey, in The Physical Basis for Heterogeneous Catalysis, eds. E. Drauglis and R. I. Jaffee (Plenum Press, 1975), p. 75.
7. S. D. Worley, N. E. Erickson, T. E. Madey, and J. T. Yates, Jr., J. Electron Spec. 9, 355 (1976).
8. J. T. Yates, Jr., T. E. Madey, N. E. Erickson, and S. D. Worley, Chem. Phys. Letters 39, 113 (1976).
9. S. D. Worley and J. T. Yates, Jr., J. Catalysis 48, 395 (1977).
10. D. W. Goodman, T. E. Madey, M. Ono, and J. T. Yates, Jr., J. Catalysis 50, 279 (1977).
11. R. D. Kelley, T. E. Madey, and J. T. Yates, Jr., J. Catalysis 50, 301 (1977).
12. J. F. Harrod, R. W. Roberts, and E. F. Rissman, J. Phys. Chem. 71, 343 (1967).
13. L. Kubelkova, P. Jiru, and P. Schurer, Collect. Czech. Chem. Comm. 34, 3842 (1969).
14. For example, see S. S. Bath and L. Vaska, J. Amer. Chem. Soc., 85, 3500 (1963); D. Evans, G. Yagupsky, and G. Wilkinson, J. Chem. Soc. A, 2660, 2665 (1968); L. Vallarino, unpublished data.
15. D. Milligan and M. Jacox, J. Chem. Phys. 41, 3032 (1964).
16. A. Adel, Phys. Rev. 45, 56 (1934).

17. For an example, see R. S. McDowell, W. D. Horrocks, Jr., and J. T. Yates, Jr., J. Chem. Phys. 34, 530 (1961).

18. F. A. Cotton and G. Wilkinson, Advanced Inorganic Chemistry, Interscience Publishers, John Wiley (1962), pp. 631-637.

19. P. S. Braterman in Structure and Bonding, Vol. 26, Eds. J. D. Dunitz, et al., Springer-Verlag, Berlin (1976), p. 32.

20. For several examples of the effect of various substituents on metal carbonyl spectra, see T. L. Brown and D. J. Darensbourg, Inorg. Chem. 6, 971 (1967).

21. For example, see P. S. Braterman, R. W. Harrill, and H. D. Kaesz, J. Amer. Chem. Soc. 89, 2851 (1967).

22. J. T. Yates, Jr., P. A. Thiel, W. H. Weinberg, Surface Science, submitted.

23. J. T. Yates, Jr., P. A. Thiel, W. H. Weinberg, Surface Science, submitted.

TABLE I

Assignment of IR Spectral Features for

Species Produced by H_2CO or CO on Rh

Species	Wavenumber (cm^{-1})	Designation
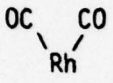	2101 (sym) 2031 (asym)	I (ref. 1)
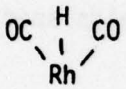	~2092 (sym) ~2025 (asym)	A
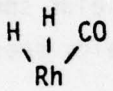	~2038	B
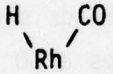	~2048	C
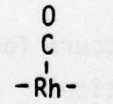	2058 - 2070	II (ref. 1)
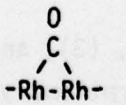	~1860	III (ref. 1)

TABLE II

Spectroscopic Observations for H_2CO Adsorption on Rh

Observation	Rationale
1. Lack of intense doublet-CO bands with H_2CO as adsorbate in contradistinction to pure CO adsorption.	1. Process (1) yields species B; CO adsorption yields species I.
2. Presence of species associated with lower $\tilde{\nu}$-CO-singlet-bands than pure CO will produce.	2. Process (1) yields species B; CO adsorption yields species II.
3. Shifted doublet produced by CO adsorption following H_2CO adsorption.	3. Process (4) yields species A; CO adsorption yields species I.
4. Interconversion of doublet-CO species to species with $\tilde{\nu}$-CO near 2048 cm^{-1} as desorption occurs.	4. Process (5) yields species C as species A loses a CO ligand.
5. Presence of an 1860 cm^{-1} species following H_2CO adsorption.	5. Process (2) occurs for both H_2CO and CO adsorption.
6. Evolution of H_2 during H_2CO adsorption/decomposition on Rh.	6. Processes (2), (3), and (4) occur for H_2CO adsorption, yielding $H_2(g)$.

Figure Captions

Figure 1. Comparison of adsorption from H_2CO and equimolar H_2 + CO on Rh. T = 295 K.

A. H_2CO Adsorption

Spectrum (a). 1.04×10^{18} H_2CO molecules added

Spectrum (b). 1.05×10^{18} H_2CO molecules added

Spectrum (c). 2.12×10^{18} H_2CO molecules added

Spectrum (d). 2.63×10^{18} H_2CO molecules added

Spectrum (e). 5.21×10^{18} H_2CO molecules added.

B. Equimolar H_2 + CO Adsorption

Spectrum (a). 1.11×10^{18} H_2 + CO molecules added

Spectrum (b). 1.09×10^{18} H_2 + CO molecules added

Spectrum (c). 2.36×10^{18} H_2 + CO molecules added

Spectrum (d). 2.75×10^{18} H_2 + CO molecules added

Spectrum (e). 5.19×10^{18} H_2 + CO molecules added

Figure 2. Site filling by CO following full coverage from H_2CO. T = 295 K.

Spectrum (a). Full coverage H_2CO followed by 60 minutes pumping.

Spectrum (b). Addition of ~50 torr CO to (a).

Figure 3. D_2CO adsorption on Rh. T = 295 K.

Spectrum (a). 1.02×10^{18} D_2CO molecules added

Spectrum (b). 1.08×10^{18} D_2CO molecules added

Spectrum (c). 2.08×10^{18} D_2CO molecules added

Spectrum (d). 2.62×10^{18} D_2CO molecules added

Spectrum (e). 5.25×10^{18} D_2CO molecules added

Figure 4. Desorption from Rh exposed to D_2CO

Spectrum (a). Full coverage of D_2CO

Spectrum (b). Follows 120 hours desorption at 295 K

Spectrum (c). Follows additional 9 hours desorption at 316 K

Lower section. Difference spectra obtained by spectrum subtraction as shown

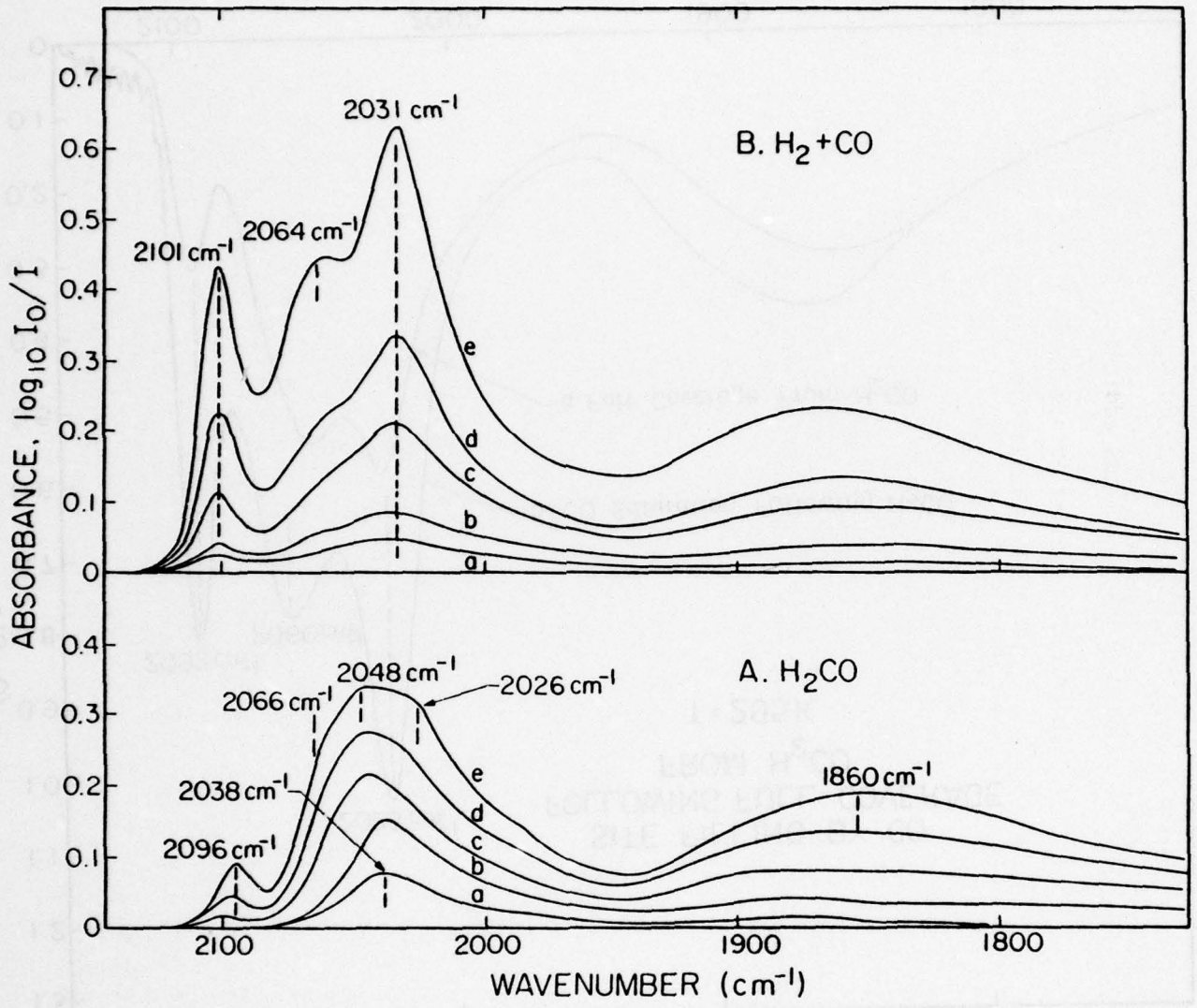
COMPARISON OF ADSORPTION FROM H_2CO AND EQUIMOLAR H_2+CO ON Rh.
B. H_2+CO
A. H_2CO
2031 cm^{-1}
2101 cm^{-1}
2064 cm^{-1}
2048 cm^{-1}
2026 cm^{-1}
2066 cm^{-1}
2038 cm^{-1}
2096 cm^{-1}
1860 cm^{-1}
a
b
c
d
e
ABSORBANCE, $\log_{10} I_0/I$
WAVENUMBER (cm^{-1})
0
0.1
0.2
0.3
0.4
0.5
0.6
0.7
2100
2000
1900
1800

Figure 1

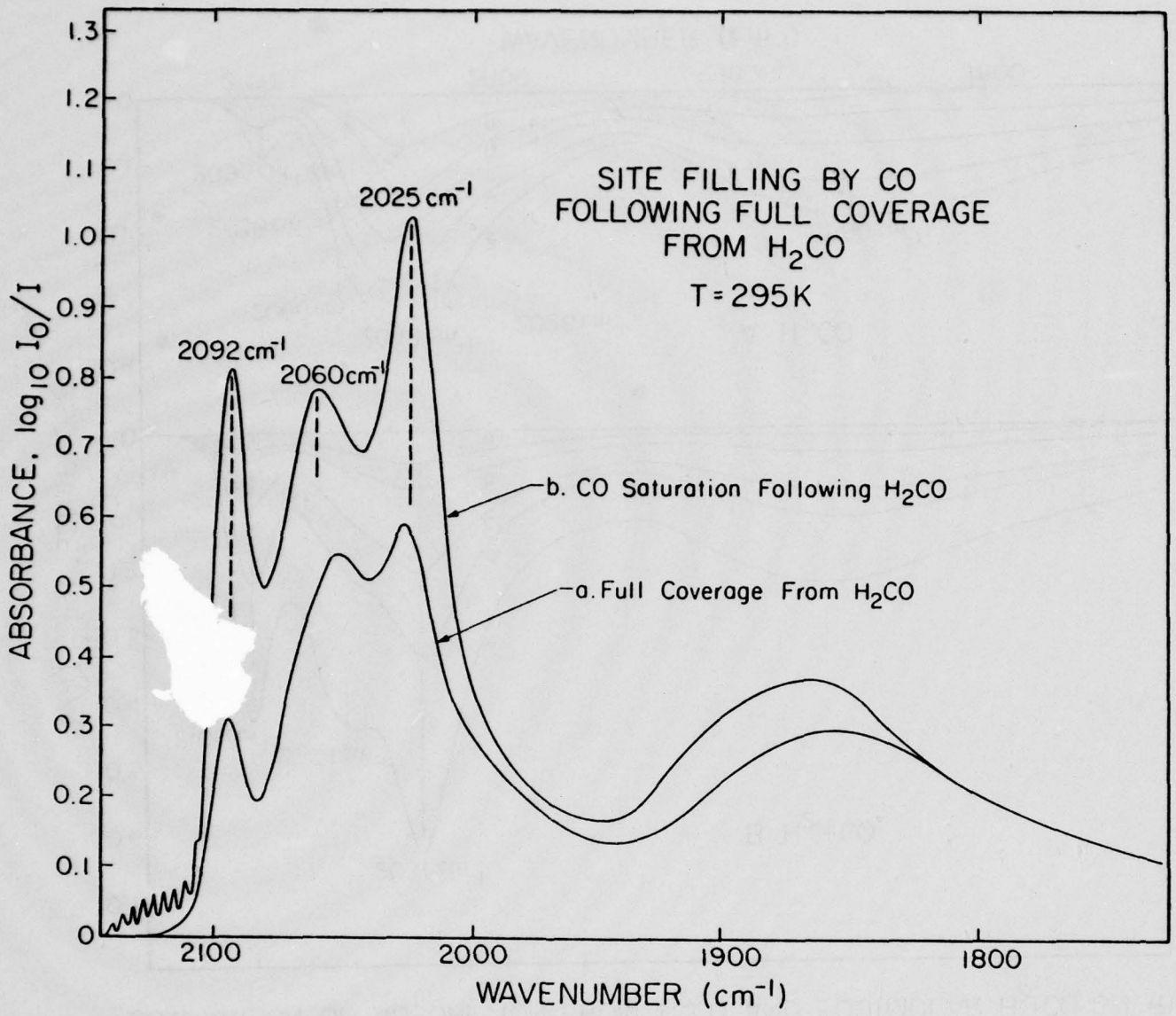
SITE FILLING BY CO
FOLLOWING FULL COVERAGE
FROM H_2CO
T = 295K
2025 cm⁻¹
2092 cm⁻¹
2060 cm⁻¹
b. CO Saturation Following H_2CO
a. Full Coverage From H_2CO
ABSORBANCE, $\log_{10} I_0/I$
WAVENUMBER (cm^{-1})
0
0.1
0.2
0.3
0.4
0.5
0.6
0.7
0.8
0.9
1.0
1.1
1.2
1.3
2100
2000
1900
1800

Figure 2

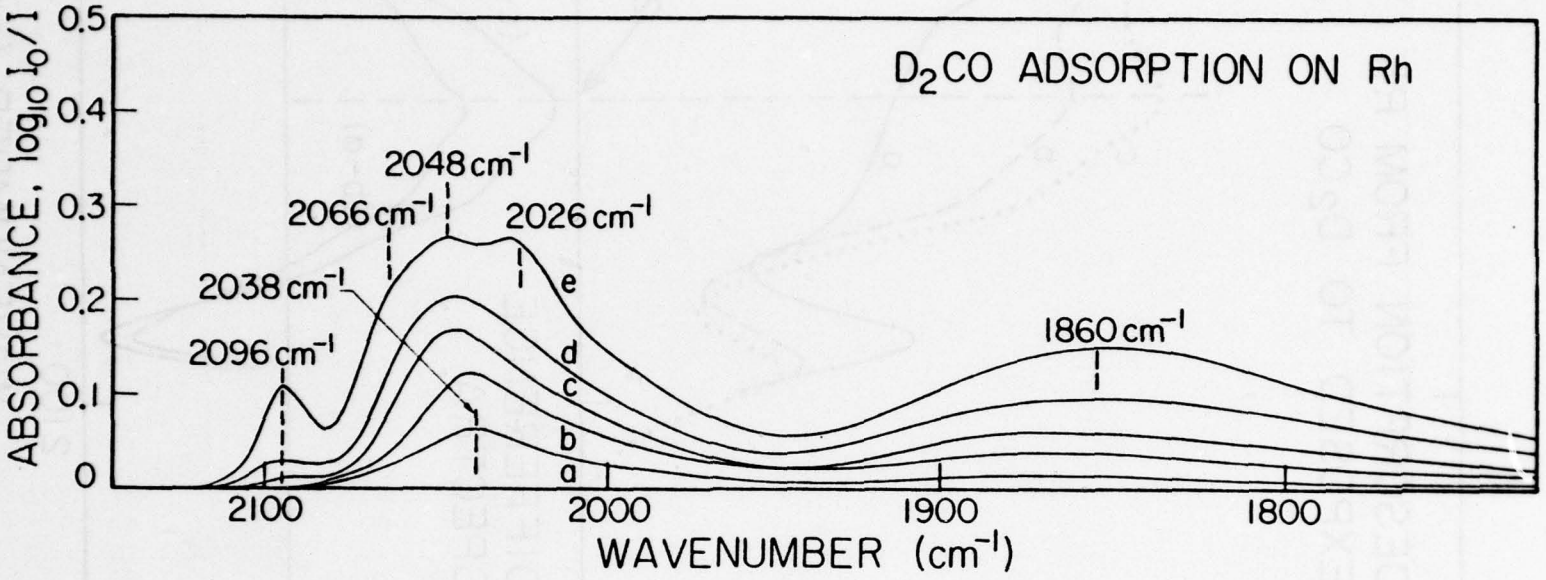
D2CO ADSORPTION ON Rh
ABSORBANCE, log10 I0/I
0.5
0.4
0.3
0.2
0.1
0
2048 cm-1
2066 cm-1
2026 cm-1
2038 cm-1
2096 cm-1
1860 cm-1
e
d
c
b
a
2100
2000
1900
1800
WAVENUMBER (cm-1)

Figure 3

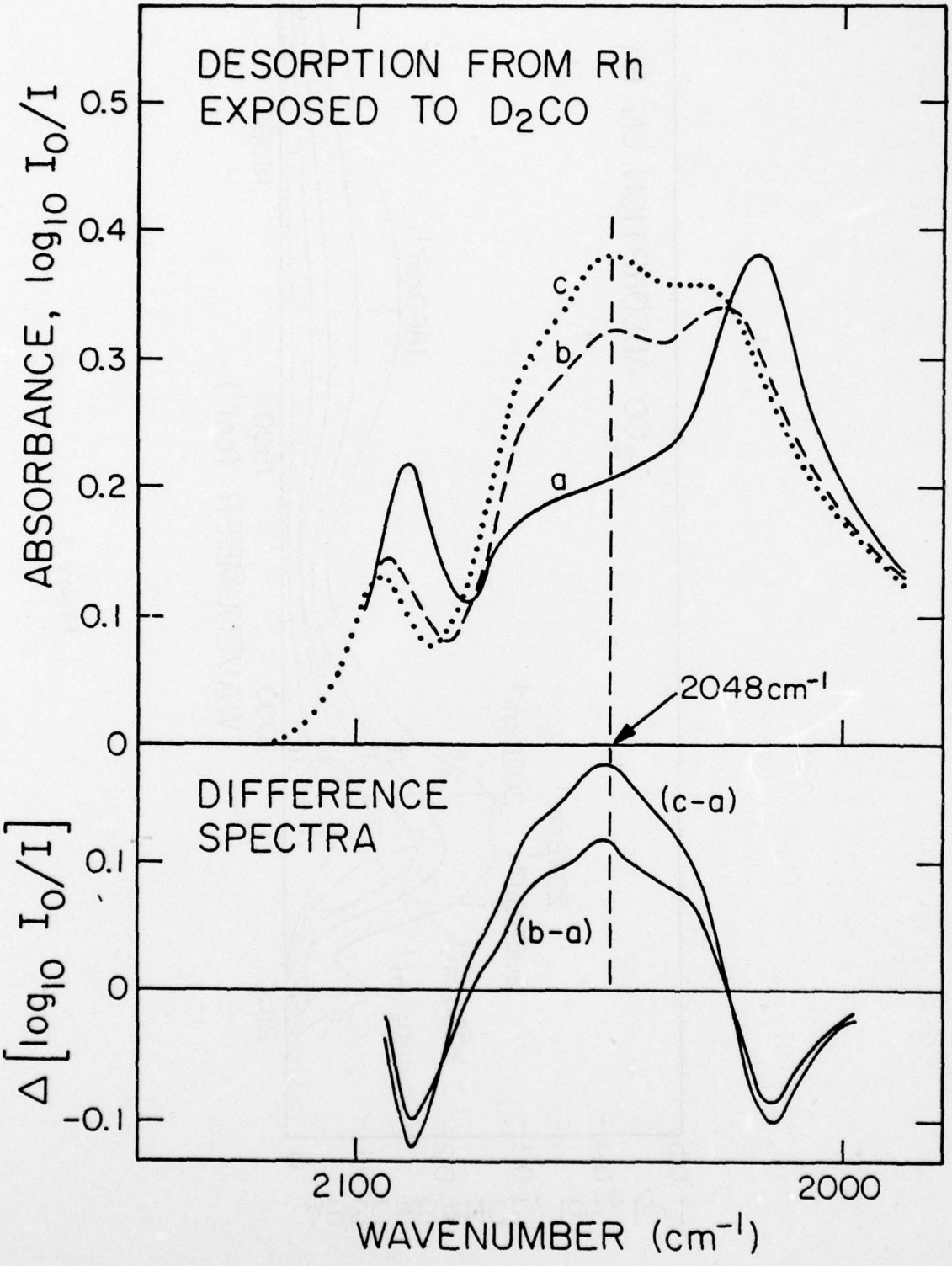
DESORPTION FROM Rh
EXPOSED TO D_2CO
ABSORBANCE, $\log_{10} I_0/I$
0.5
0.4
0.3
0.2
0.1
0
c
b
a
2048cm^{-1}
DIFFERENCE
SPECTRA
$\Delta[\log_{10} I_0/I]$
0.1
0
-0.1
(c-a)
(b-a)
2100
2000
WAVENUMBER (cm^{-1})

Figure 4